

# Ochratoxin A, citrinin and deoxynivalenol decrease claudin-2 expression in mouse rectum CMT93-II cells

Hideaki Nakayama, Norio Kitagawa, Takahito Otani, Hiroshi Iida, Hisashi Anan, Tetsuichiro Inai

## Abstract

Intestinal epithelial cells are the first targets of ingested mycotoxins, such as ochratoxin A, citrinin, and deoxynivalenol. It has been reported that paracellular permeability regulated by tight junctions is modulated by several mycotoxins by reducing the expression of specific claudins and integral membrane proteins in cell-cell contacts, accompanied by increase in phosphorylation of mitogen-activated protein kinases, including extracellular signal-related kinase (ERK) 1/2, p38, and c-Jun NH<sub>2</sub>-terminal protein kinase. Claudin-2 is expressed in the deep crypt cells, but not in the villus/surface cells in vivo. While Caco-2, T84, and IPEC-J2 cells, which are widely used intestinal epithelial cell lines to assess the influence of mycotoxins, do not express claudin-2, CMT93-II cells express claudin-2. We previously reported that inhibition of the ERK pathway reduced claudin-2 levels in cell-cell contacts in CMT93-II cells. In this study, we examined whether ochratoxin A, citrinin, and deoxynivalenol affect claudin-2 expression and ERK1/2 phosphorylation in CMT93-II cells. We found that all mycotoxins reduced claudin-2 expression in cell-cell-contacts, with reduction (by citrinin and deoxynivalenol) or no change (by ochratoxin A) in phosphorylated ERK1/2. All mycotoxins increased transepithelial electrical resistance, but did not affect flux of fluorescein. While ochratoxin A and citrinin are known to be nephrotoxic, only deoxynivalenol reduced claudin-2 expression in MDCK II cells derived from the renal tubule. These results suggest that claudin-2 expression is regulated not only by the ERK pathway, but also by other pathways in an organ-specific manner.

## Introduction

Mycotoxins are toxic secondary metabolites produced by different fungi that can cause health problems in humans and farm animals. The chemical structures of mycotoxins vary considerably, but they are low molecular mass organic compounds [1]. Most of the mycotoxins are produced by fungi belonging to the species *Aspergillus*, *Penicillium*, and *Fusarium*. For example, ochratoxin A (OTA), citrinin (CTN), and deoxynivalenol (DON) are produced by *Aspergillus ochraceus*, *Penicillium citrinum*, and *Fusarium graminearum* [2], respectively. Exposure to mycotoxins is mostly by ingestion, but also occurs by dermal, respiratory, and parental routes. It is reported that about 25% of the world's crop production may be contaminated by mycotoxins [3]. Thus, it is most likely that mycotoxins enter the

body through the epithelium of the digestive tract. These mycotoxins then spread throughout the body via the blood stream. In fact, OTA has been shown to be absorbed passively throughout the gastrointestinal tract, especially the stomach and jejunum [4, 5], and has been detected in the blood [1] as well as human milk [6-9]. The mycotoxins spread throughout the body and affect specific organs by an unknown mechanism. OTA and CTN affect the kidney, and are thus known as nephrotoxins [10]. DON belongs to the trichothecenes family of mycotoxins. Acute toxicity of trichothecenes induces diarrhea, vomiting, leukocytosis, and hemorrhage, while chronic toxicity of trichothecenes causes weight loss and neuroendocrine and immunological changes [11].

Substances pass through the epithelia via two routes, paracellular and transcellular routes. Tight junctions are located in the most apical portion of the lateral plasma membrane of epithelial cells and restrict the passage of ions, solutes, and macromolecules between adjacent cells (paracellular route). Tight junctions are formed by integral membrane proteins, such as claudins [12], occludin [13], junctional adhesion molecule [14], tricellulin [15], and MarvelD3 [16] and scaffolding proteins, such as ZO proteins [17-19], which link actin filaments to tight junctions. The claudin family consists of at least 27 members [20] and forms the backbone of tight junctions. Claudin-1, -3, and -5 are sealing claudins, which increase the tightness of the barrier [21-23]. Some claudins form paracellular channels whose cation- or anion-selectivity depends on the net charge of the second half of extracellular loop 1 of each claudin [24]. While claudin-2, -10b, and -15 form cation-selective channels [25-30], claudin-10a and -17 form anion-selective channels [29, 31].

In vitro studies using human and piglet intestinal epithelial cell lines have shown that both OTA and DON induce an increase in paracellular permeability, accompanied by reduction in the protein expression of specific claudins [32-39]. Treatment with DON increases phosphorylation of mitogen-activated protein kinases (MAPKs), including extracellular signal-related kinase (ERK) 1/2, p38 MAPK, and c-Jun NH<sub>2</sub>-terminal protein kinase (JNK) [36, 38, 39]. The effect of CTN on claudins expression in intestinal epithelial cells has not been studied so far.

Claudins are localized in different segments of the intestine, such as the duodenum, jejunum, ileum, and large intestine (for review, see Lu *et al.* [40]). Furthermore, several claudins show selective expression along the crypt-villus axis in the small intestine and crypt-surface axis in the large intestine. For example, claudin-2 is localized in the deep crypt of the intestine [41, 42]. Thus, if mycotoxins influence the expression of specific claudin isoform(s), segment-specific and crypt-villus/surface axis-specific alteration of paracellular permeability may be caused by mycotoxins depending on which claudins are expressed in the intestinal epithelial cells. Since CMT93-II cells, a clone of CMT93 cells derived from mouse rectum carcinoma [43], express claudin-2 protein [44], these cells exhibit the features of deep crypt cells. In contrast, differentiated Caco-2 and T84 cells, which are widely used as models

for the intestinal barrier, hardly express claudin-2 [35, 41, 45], and thus exhibit the features of intestinal villus/surface cells. We previously reported that claudin-2 protein expression was positively or negatively regulated by ERK1/2 depending on the cell type [46].

In this study, using CMT93-II cells, which are different from the previously reported intestinal epithelial cells with regard to claudin expression patterns, we examined whether mycotoxins (OTA, CTN, and DON) affect paracellular permeability, phosphorylation of MAPKs, and expression of claudins, especially claudin-2. Because OTA and CTN are nephrotoxic [10], we examined if they influence claudin-2 protein expression in Madin-Darby canine kidney (MDCK) II cells, which are derived from the distal tubule or collecting duct of the nephron.

## **Methods**

### ***Reagents***

OTA and CTN were purchased from Enzo Life Sciences (Farmingdale, NY, USA). DON was obtained from Cayman Chemical (Ann Arbor, MI, USA). U0126 and SB202190 were obtained from Sigma-Aldrich (Saint Louis, MO, USA). Stock solutions of OTA (50 mM), CTN (50 mM), DON (20 mM), U0126 (20 mM), and SB202190 (40 mM) in dimethylsulfoxide (DMSO) were prepared.

### ***Cell culture and treatment with mycotoxins or U0126***

CMT93-II and MDCK II Tet-Off cells (Clontech, Palo Alto, CA, USA) were grown in Dulbecco's modified Eagle medium (DMEM) supplemented with 10% fetal bovine serum, 2 mM glutamine, 100 U/mL penicillin, and 100 µg/mL streptomycin (Gibco, Grand Island, NY, USA). The cells were treated with vehicle (DMSO), mycotoxins, or U0126 at the indicated concentration for the indicated time periods.

### ***Immunofluorescence microscopy***

CMT93-II and MDCK II Tet-Off cells were seeded at a density of  $3.0 \times 10^4$  and  $6.0 \times 10^4$  cells/well, respectively, in the wells (6 mm in diameter) of 10-well glass slides printed with highly water-repellent marks (Matsunami Glass Ind. Ltd., Osaka, Japan). Next day, when the cells reached confluence, they were treated with 40 µM OTA for CMT93-II cells, 10 µM OTA for MDCK II cells, 50 µM CTN, 1 µM DON, 20 µM U0126, 20 µM SB202190, or 0.1% DMSO (vehicle) for 36 h. They were fixed with 1% paraformaldehyde in phosphate buffered saline (PBS) for 10 min, washed in PBS, incubated in 0.2% Triton-X 100 in PBS for 10 min, washed again in PBS, and then incubated with 1% bovine serum albumin in PBS (BSA-PBS) for 30 min at room temperature to block non-specific binding. The samples were incubated with primary antibodies for 1 h in a moist chamber. Primary antibodies against claudin-2 (1:100), claudin-4 (1:200), claudin-6 (1:100), and GATA-4 (1:50) were purchased from

Zymed (South San Francisco, CA, USA), Abcam (Cambridge, MA, USA), IBL (Takasaki, Japan), and Santa Cruz (Santa Cruz, CA, USA), respectively. After rinsing in PBS five times for 3 min each, samples were incubated with secondary antibodies at a 1:400 dilution in BSA-PBS for 30 min in the dark. Anti-mouse Ig and anti-rabbit Ig conjugated with either Alexa 488 or Alexa 594 (Molecular Probes, Eugene, OR, USA) were used as secondary antibodies. Cells were then washed five times in PBS for 3 min each, and mounted in Vectashield mounting medium containing 4',6-diamidino-2-phenylindole (DAPI; Vecta Laboratories, Burlingame, CA, USA). The specimens were examined under a Zeiss LSM 510 confocal microscope (Oberkochen, Germany).

### ***Gel electrophoresis and immunoblot analysis***

Confluent cells cultured on 35-mm culture dishes were treated with vehicle, mycotoxins, or U0126 as described in the above section. Cells were washed with ice-cold PBS and lysed in lysis buffer [62.5 mM Tris, pH 6.8, 2% sodium dodecyl sulfate (SDS), 10% glycerol, 5% 2-mercaptoethanol, and 0.002% bromophenol blue] containing protease inhibitor cocktail (Sigma-Aldrich) and phosphatase inhibitor cocktail (Nacalai Tesque, Kyoto, Japan). Cell lysates (5 $\mu$ L per lane) were fractionated by SDS-polyacrylamide gel electrophoresis (PAGE) and then transferred onto polyvinylidene difluoride (PVDF) membranes. Precision Plus protein dual color standards (Bio-Rad, Hercules, CA, USA) were used to calculate the size of the detected bands. The membranes were incubated with Blocking One (Nacalai Tesque, Kyoto, Japan) for 1 h and then with primary antibodies (listed below) overnight at 4°C. Antibodies against phospho (P)-ERK (1:1,000), ERK (1:1,000), P-p38 (1:1,000), p38 (1:1,000), P-JNK (1:1,000), JNK (1:1,000), actin (1:2,000), claudin-2 (1:1,000), claudin-4 (1:1,000), and claudin-6 (1:1,000) were used as primary antibodies and diluted with Tris buffered saline (TBS) [20 mM Tris (pH 7.6) and 137 mM NaCl] containing 5% Blocking One. These primary antibodies against MAPKs were obtained from Cell Signaling Technology (San Diego, CA, USA) and anti-actin antibody was from Sigma-Aldrich. After washing with TBS containing 0.1% Tween 20 (T-TBS), cells were incubated with horseradish peroxidase (HRP)-conjugated anti-rabbit or anti-mouse Ig (1:2,000) (GE Healthcare UK Ltd, Buckinghamshire, England) for 1 h. They were then washed with T-TBS and the bands were detected using Luminata Forte Western HRP substrate (Millipore, Billerica, MA, USA). Some membranes were reprobated after stripping primary and secondary antibodies with stripping buffer [62.5 mM Tris (pH 6.7), 2% SDS, and 100 mM 2-mercaptoethanol] at 50°C for 30 min.

### ***RNA extraction and quantitative polymerase chain reaction (qPCR)***

CMT93-II cells ( $1 \times 10^6$  cells/well) and MDCK II cells ( $2 \times 10^6$  cells/well) were seeded onto 6-well plates and treated with 40  $\mu$ M OTA for CMT93-II cells, 10  $\mu$ M OTA for MDCK II

cells, 50  $\mu$ M CTN, 1  $\mu$ M DON, 20  $\mu$ M U0126, or 0.1% DMSO (vehicle) for 36 h. RNA extraction and qPCR were performed according to the manufacturer's instructions. Briefly, total RNA was extracted using SV total RNA isolation system (Promega, Madison, WI, USA). Reverse transcription and amplification were carried out using the GoTaq 2-Step RT-qPCR system (Promega, Madison, WI, USA). Relative mRNA levels were measured with a SYBR Green detection system using the 7500 real-time PCR system (Applied Biosystems, Foster City, CA). All samples were measured in triplicate. The relative mRNA level of each gene was calculated as the ratio of target to control gene ( $\beta$ -actin). The following PCR primers were used: mouse  $\beta$ -actin [47]: forward, 5'-AGA GGG AAA TCG TGC GTG AC-3' and reverse, 5'- CAA TAG TGA TGA CCT GGC CGT-3'; mouse claudin-2 [48]: forward, 5'- TAT GTT GGT GCC AGC ATT GT-3' and reverse, 5'-TCA TGC CCA CCA CAG AGA TA-3'; mouse claudin-4 [32]: forward, 5 -CGC TAC TCT TGC CAT TAC G-3' and reverse, 5'-ACT CAG CAC ACC ATG ACT TG-3'; mouse claudin-6 [49]: forward, 5'-GCA GTC TCT TTT GCA GGC TC-3' and reverse, 5'-CCC AAG ATT TGC AGA CCA GT-3'; canine  $\beta$ -actin [50]: forward, 5'-CGA GAC ATT CAA CAC CCC AAC-3' and reverse, 5'-AGC CAG GTC CAG ACG CAA G-3'; canine claudin-2 [51]: forward, 5'-GGT GGG CAT GAG ATG CAC T-3' and reverse, 5'-CAC CAC CGC CAG TCT GTC TT-3'. The specificity of the amplified products was evaluated by melting curve analysis.

#### ***Measurement of transepithelial electrical resistance (TER)***

CMT93-II cells were seeded at  $6.0 \times 10^4$  cells/wells on 12-mm membrane culture inserts (Millicell-HA; Millipore, Bedford, MA, USA) in a 24-well plate, and cultured to confluence for 4 days. Culture medium containing vehicle, 100  $\mu$ M OTA, 125  $\mu$ M CTN, or 2.5  $\mu$ M DON was added to the apical compartment and the cells were cultured for 48 h. During this period, TER was measured with a Millicell ERS-2 epithelial voltohmmeter (Millipore), as described previously [52]. To examine the effect of  $\text{Na}^+$ , some of the TER measurements were performed in  $\text{P}_{\text{Na}}$  buffer containing 140 mM sodium aspartate, 2 mM  $\text{CaCl}_2$ , 1 mM  $\text{MgCl}_2$ , 10 mM glucose, 10 mM HEPES, pH7.3 [53]. The TER values were calculated by subtracting the contribution of the bare filter and medium and multiplying it by the surface area of the filter. All experiments were performed twice in triplicate.

#### ***Measurement of paracellular permeability***

CMT93-II cells were seeded and treated with mycotoxins for 48 h, as described in the above section. Inserts and wells were washed three times with P buffer [10 mM HEPES (pH 7.4), 1 mM sodium pyruvate, 10 mM glucose, 3 mM  $\text{CaCl}_2$ , and 145 mM  $\text{NaCl}$ ]. P buffer with or without 30  $\mu$ g/mL fluorescein (Sigma-Aldrich) was added to the upper or lower compartment, respectively. The P buffer from the lower compartment was collected at 2 h after addition of the tracer, and paracellular flux was measured with a fluorometer (excitation, 492 nm;

emission, 520 nm). Experiments were performed twice in triplicate.

### ***Statistical analysis***

All data are expressed as the mean  $\pm$  standard error of mean (SEM). Statistical differences between groups were determined by the two-sided Welch's *t*-test.  $P < 0.05$  was considered statistically significant.

### **Results**

We first determined the concentration that affected the expression of claudin-2, -4, or -6 in cell-cell contacts in CMT93-II cells. In previous reports, intestinal epithelial cells were treated with 1–100  $\mu$ M of OTA [34, 35, 54, 55] or 1–100  $\mu$ M of DON [32, 36, 37, 54]. Although there is no data of CTN treatment of intestinal epithelial cell lines, CTN was used at concentration of 30  $\mu$ M or 50  $\mu$ M in kidney PK15 cells [56]. We first tested 1, 5, 10, 20, 50, and 100  $\mu$ M of each mycotoxin for 48 h and examined the localization of claudins. Then, the concentration was reduced by 10  $\mu$ M or 1  $\mu$ M. We selected 40  $\mu$ M OTA, 50  $\mu$ M CTN, and 1  $\mu$ M DON to treat cells without obvious cell damage. Localization of claudin-2, -4, and -6 after treatment with mycotoxins or U0126 was examined by confocal microscopy (Fig. 1). Localization of claudin-2 in cell-cell contacts was significantly reduced by treatment with OTA, CTN, and DON (Fig. 1) as well as 20  $\mu$ M U0126, as previously reported [46]. Localization of claudin-4 and -6 was not affected by mycotoxins and U0126, though OTA slightly reduced claudin-4 staining in cell-cell contacts. Next, we examined the total protein expression of claudins and phosphorylation of MAPKs, including ERK1/2, p38, and JNK by immunoblotting (Fig. 2). Consistent with microscopy data, claudin-2 protein expression was prominently reduced by treatment with all mycotoxins and U0126, while that of claudin-4 was prominently reduced by OTA. Although there was no clear reduction in claudin-4 and -6 expression in cell-cell contacts by DON treatment when examined by confocal microscopy, immunoblotting revealed that claudin-4 expression was slightly reduced, and claudin-6 expression was considerably reduced by DON. Phosphorylation of JNK was neither detected in control cells nor in cells treated with mycotoxins or U0126. Phosphorylation of ERK1/2 was clearly reduced by CTN, DON, and U0126, but was not altered by OTA. Phosphorylation of p38 was slightly increased by OTA and CTN, but decreased by DON and U0126. Treatment of SB202190, an inhibitor of p38 MAPK, did not alter localization of claudin-2 and claudin-4 at sites of cell-cell contact between CMT93-II cells (Supplementary Fig. 1). The transcription factor GATA-4 was detected in the nucleus of CMT93-II cells but not in that of MDCK II cells (Supplementary Fig. 2). Treatment of CMT93-II cells with OTA, CTN, DON, and U0126 decreased claudin-2 in cell-cell contacts, but GATA-4 was still detected in their nucleus (Supplementary Fig. 2).

We examined the relative mRNA level of expression of claudin-2, -4, and -6

standardized by  $\beta$ -actin (Fig. 3). Claudin-2 mRNA was markedly decreased by OTA, CTN, DON, and U0126. Claudin-4 transcript was slightly decreased by U0126, significantly decreased by OTA and CTN, and significantly increased by DON. Claudin-6 transcript was slightly decreased by DON and U0126, and clearly decreased by OTA and CTN. The decreased expression level of claudin-2 transcript in cells treated with OTA, CTN, DON, and U0126 (Fig. 3) was consistent with the decreased expression level of claudin-2 protein (Fig. 2). However, the expression level of transcripts was not always consistent with that of proteins. For example, while expression of claudin-4 transcript was decreased by CTN or increased by DON (Fig. 3), that of claudin-4 protein was unaffected by CTN or slightly decreased by DON (Fig. 2).

Next, we examined whether treatment with mycotoxins affected paracellular permeability by assessing TER and flux of fluorescein. TER represents the instantaneous electrical conductance of soluble ions, while flux assesses the amount of large non-charged molecules passed through transient breaks in anastomosing tight junction strands usually over one hour or more. Culture medium containing vehicle (0.25% DMSO), 100  $\mu$ M OTA, 125  $\mu$ M CTN, or 2.5  $\mu$ M DON was added to the apical compartment because ingested mycotoxins first come in contact with the apical membrane domain of intestinal epithelial cells. The apical and basal compartment contained 0.4 and 0.6 mL of culture medium, respectively. If mycotoxins were diluted with the total volume of the medium (1.0 mL), the final concentration became the same as the concentration that was used in cells seeded in 10-well glass slides for confocal microscopy. Therefore, we used 2.5 times higher concentration of mycotoxins than that used for confocal microscopy. Similarly, a higher concentration of U0126 was required to induce an increase in TER and decrease in claudin-2 protein expression in CMT93-II cells seeded on membrane culture inserts [46]. TER in cells treated with OTA, CTN, or DON for 24 h was approximately 2 times higher than that in control cells (Fig. 4A). At 48 h, TER in cells treated with OTA, CTN, or DON was 1.6, 2, or 1.7 times higher than that in control cells, respectively (Fig. 4A).  $P_{Na}$  buffer principally contains sodium aspartate ( $Na^+$ , aspartate $^-$ ) to examine the effect of  $Na^+$  on TER. After treatment of OTA, CTN, or DON for 48 h, TER was measured in  $P_{Na}$  buffer. In  $P_{Na}$  buffer, increased TER was observed in cells treated with OTA, CTN, or DON, indicating the decrease of paracellular permeability for  $Na^+$ , thereby increasing TER (Fig. 4B). Fluorescein was used as a tracer to assess paracellular permeability. The molecular weight of fluorescein is 332.3, which is close to that of OTA (403.8), CTN (250.2), and DON (296.3). In spite of the increase in TER by all mycotoxins, flux of fluorescein remained unaltered (Fig. 5).

Finally, we examined whether treatment with OTA, CTN, DON, and U0126 influenced expression of claudin-2 in MDCK II cells derived from the dog renal tubule, because OTA and CTN are known to be nephrotoxic. Although DON markedly reduced claudin-2 localization in cell-cell contacts, OTA, CTN, and U0126 did not alter the

localization of claudin-2 (Fig. 6A). Consistently, DON markedly reduced claudin-2 protein (Fig. 6B) and mRNA (Fig. 6C). Findings from the present and previous studies regarding the effects of DON, OTA, and CTN on the intestinal cell lines, jejunal explants, or MDCK II cells are summarized in Table 1.

## Discussion

In this study, we showed that OTA, CTN, or DON treatment increased TER in CMT93-II cells by reducing paracellular permeability for Na<sup>+</sup>, concomitant with marked reduction of claudin-2 expression in cell-cell contacts. Claudin-2 forms cation-permeable paracellular channels [24, 25, 30, 57] in tight junctions, thereby inducing reduction in TER in claudin-2-overexpressing epithelial cells. Conversely, it is likely that removal of claudin-2 from tight junctions induces an increase in TER. In fact, treatment of CMT93-II cells with U0126, an inhibitor of the ERK pathway, reduced claudin-2 expression in cell-cell contacts and increased TER [46]. Several studies have examined the effects of DON and OTA on TER in human intestinal epithelial cell lines (Caco-2, T84, and HT-29) [32-35, 37, 54, 58, 59] or piglet intestinal epithelial cell lines (IPEC-1 and IPEC-J2) [36-39, 60]. Inconsistent with our result, both DON and OTA induced reduction in TER in these intestinal cell lines. This discrepancy can be explained by the different expression patterns of claudins among the different intestinal epithelial cell lines examined. IPEC-J2 cells express claudin-1, -3, -4, -5, -7, -8, and -12 proteins as demonstrated by immunoblotting [61], but do not express claudin-2 and -15 [62]. Although Caco-2 cells express claudin-2 in cell-cell contacts before they reach confluence, the expression is markedly reduced after confluence [35, 41]. Because TER was examined in differentiated Caco-2 cells after confluence in all previous reports, claudin-2 was hardly expressed. Similarly, claudin-2 expression was abolished in cell-cell contacts in T84 cells after confluence [45]. Taken together, OTA, CTN, and DON increased TER by removing claudin-2 from tight junctions in CMT93-II cells.

qPCR analysis revealed that all mycotoxins and U0126 markedly reduced claudin-2 transcripts, suggesting that all mycotoxins as well as inhibition of the ERK pathway reduced claudin-2 levels in cell-cell contacts by reducing the expression of claudin-2 transcripts. Consistent with our results, the level of claudin-4 transcript was decreased by OTA [55]. While claudin-4 transcript levels in CMT93-II cells treated with DON were 1.4 times higher than that in control cells, claudin-4 protein level was paradoxically decreased. A similar discrepancy was reported previously in Caco-2 cells treated with DON [32]. Although further studies are needed, DON treatment may suppress translation and/or increase degradation of claudin-4 protein.

Confocal microscopy showed that OTA, CTN, and DON removed claudin-2 from cell-cell contacts in CMT93-II cells and that OTA slightly reduced claudin-4 expression in cell-cell contacts. Immunoblot analysis confirmed the reduction in claudin-2 expression, and

also revealed the reduction in claudin-4 and -6 expression by DON treatment, even though continuous immunofluorescence staining for claudin-4 and -6 was detected in cell-cell contacts. Consistently, claudin-4 level was decreased by OTA and DON in Caco-2 and IPEC-1 cells [33-36, 38]. However, claudin-4 protein expression was not altered by DON treatment in IPEC-J2 cells, but claudin-1 and -3 levels were decreased [39]. It is debatable whether claudin-4 acts as a sealing claudin (barrier against Na<sup>+</sup> and Cl<sup>-</sup>) or not. Claudin-4 was previously reported to act as a sealing claudin [63]. Later, claudin-4 was found to act as a Na<sup>+</sup> barrier without affecting Cl<sup>-</sup> permeability [24, 64], or as an anion channel when it was expressed with claudin-8 [65]. Claudin-6 was shown to act as a sealing claudin when overexpressed in MDCK II cells expressing claudin-2 [66]. Although CTN reduced only claudin-2 levels, OTA or DON reduced claudin-4 or claudin-4 and -6 levels, respectively, in addition to reduction of claudin-2 level. Therefore, claudin-4 and -6 may act as sealing claudins in CMT93-II cells because the increase in TER by OTA and DON was lesser than that by CTN.

Claudin isoforms distribute differently in the gastrointestinal tract (for review, see Lu *et al.* [40]). In mice, for example, claudin-2, -3, -7, and -15 have been shown to localize in all segments of the small (duodenum, jejunum, and ileum) and large intestine. Claudin-12 is distributed in the jejunum, ileum, and large intestine. Claudin-1, -4, and -8 have been detected in the ileum and large intestine. Claudin-5 and -13 are restricted to the large intestine. Intestinal epithelial cells differentiate and move from the crypt to the villus (small intestine) or surface (large intestine). Along these axes, claudin-2 is restricted to the deep crypt in the intestine [41, 42]. Therefore, intestinal epithelial cells express different combinations and mixing ratios of claudin isoforms, not only in the intestinal segment, but also along the crypt-villus/surface axis. It is possible that each claudin isoform expressed in intestinal epithelial cells can be differently affected by mycotoxins. If this is true, mycotoxins differently modulate paracellular permeability in the intestinal segment and along the crypt-villus/surface axis. CMT93-II cells have the features of deep crypt cells because CMT93-II cells expresses claudin-2 [44]. It is speculated that intestinal epithelial cells in the deep crypt *in vivo* may increase TER via removal of cation-selective channels formed by claudin-2 after treatment with OTA, CTN, and DON.

Because DON activates MAPKs in pig intestinal epithelial cells *in vitro* [36, 38, 39] and in porcine jejunal explants [67], we examined phosphorylation of MAPKs in CMT93-II cells treated with OTA, CTN, and DON. Although DON binds to the ribosomes and activates ERK1/2 and p38, known as the ribotoxic stress response [68], treatment with 1 μM DON decreased phosphorylation of ERK1/2 and p38 in CMT93-II cells. In porcine intestinal epithelial cells, treatment with 10–30 μM DON increased phosphorylation of MAPKs [36, 38, 39]. In jejunal explants, 10 μM DON increased phosphorylation of ERK1/2 and p38, while 5 μM DON had no effect [67]. In contrast to porcine intestinal epithelial cells and jejunal

explants, 1  $\mu$ M DON decreased phosphorylated ERK1/2 in CMT93-II cells. We previously reported that inhibition of the ERK1/2 pathway by U0126 removed claudin-2 from cell-cell contacts in CMT93-II cells and increased TER [44]. Therefore, DON and CTN may reduce claudin-2 levels through suppression of ERK1/2 phosphorylation in CMT93-II cells. OTA did not alter the phosphorylation of ERK1/2, but reduced claudin-2 level in cell-cell contacts, suggesting that more than two pathways, including the ERK pathway may regulate the localization of claudin-2 in cell-cell contacts in CMT93-II cells. DON, but not OTA, CTN, and U0126, decreased claudin-2 levels in cell-cell contacts in MDCK II cells derived from the renal tubule, suggesting that claudin-2 expression is regulated in an organ-specific manner (intestine versus kidney). Moreover, reduction in claudin-2 expression was induced by inhibition of the ERK pathway in intestinal epithelial cells, such as T84 [69] and CMT93-II cells [46] or, on the contrary, by activation of the ERK pathway in renal tubule-derived MDCK II cells [70]. In our next study, we aim to examine whether DON affects ERK1/2 phosphorylation in MDCK II cells.

The precise mechanism underlying the decrease in claudin-2 levels in cell-cell contacts by OTA, CTN, and DON in CMT93-II cells is still unclear; however, involvement of the CNT- and DON-mediated inhibition of the ERK pathway is suggested in this study. The decrease in claudin-2 mRNA expression, induced by OTA, CTN, and DON, is one of the reasons for the decreased claudin-2 protein localization in cell-cell contacts. Inhibition of the p38 pathway by SB202190 did not decrease claudin-2 protein localization in cell-cell contacts in CMT93-II cells (Supplementary Fig. 1), suggesting that decrease in claudin-2 localization may not be induced by the decrease in phosphorylated p38 levels on treatment with DON and U0126 (Fig. 2). We examined the nuclear localization of GATA-4, a transcription factor related to maintenance of claudin-2 protein expression in the intestine but not in the kidney [41], in CMT93-II cells treated with OTA, CTN, and DON, but GATA-4 was still detected in their nucleus (Supplementary Fig. 2). Thus, GATA-4 may not be involved in maintenance of claudin-2 expression in CMT93-II cells. Claudin-2 is continuously endocytosed and recycled back to plasma membrane, and inhibition of this process causes reduction of claudin-2 in cell-cell contacts [71, 72]. In autophagy-induced Caco-2 cells, claudin-2 is targeted to the lysosome; consequently, its levels are decreased in cell-cell contacts [73]. In our future study, we will examine whether endocytosis and/or autophagy is related to decreased claudin-2 localization at sites of cell-cell contact between CMT93-II cells treated with mycotoxins.

### **Concluding remarks**

In this study, we showed that treatment with mycotoxins (OTA, CTN and DON) induced a decrease in the level of claudin-2, which forms cation-selective channels in cell-cell contacts, and an increase in TER, but did not alter flux of fluorescein in CMT93-II cells. Treatment with U0126, a specific inhibitor of the ERK pathway, also decreased claudin-2 level in

cell-cell contacts and increased TER. While CTN and DON decreased the phosphorylation of ERK1/2, OTA did not alter it. Therefore, more than two pathways, including the ERK pathway may regulate claudin-2 expression in cell-cell contacts. As claudin-2 localizes in the deep crypt, it is possible that mycotoxins may differently modulate paracellular permeability of ions along the crypt-villus/surface axis. Paracellular permeability of enterocytes may be differently modulated by mycotoxins, which decrease the levels of specific claudin isoforms depending on which isoform they express.

### Acknowledgements

We thank Dr. Ishii (Fukuoka Dental College) for providing technical advice to do qPCR.

### References

1. Peraica M, Radic B, Lucic A, and Pavlovic M (1999) Toxic effects of mycotoxins in humans. *Bull. World Health Organ.* 77: 754–766.
2. Kushiro M (2008) Effects of milling and cooking processes on the deoxynivalenol content in wheat. *Int. J. Mol. Sci.* 9: 2127–2145.
3. Oswald I P, Marin D E, Bouhet S, Pinton P, Taranu I, and Accensi F (2005) Immunotoxicological risk of mycotoxins for domestic animals. *Food Addit. Contam.* 22: 354–360.
4. Kumagai S, and Aibara K (1982) Intestinal absorption and secretion of ochratoxin A in the rat. *Toxicol. Appl. Pharmacol.* 64: 94–102.
5. Roth A, Chakor K, Creppy E E, Kane A, Roschenthaler R, and Dirheimer G (1988) Evidence for an enterohepatic circulation of ochratoxin A in mice. *Toxicology* 48: 293–308.
6. Marquardt R R, and Frohlich A A (1992) A review of recent advances in understanding ochratoxicosis. *J. Anim. Sci.* 70: 3968–3988.
7. Micco C, Miraglia M, Brera C, Corneli S, and Ambrozzi A (1995) Evaluation of ochratoxin A level in human milk in Italy. *Food Addit. Contam.* 12: 351–354.
8. Munoz K, Blaszkewicz M, Campos V, Vega M, and Degen G H (2014) Exposure of infants to ochratoxin A with breast milk. *Arch Toxicol.* 88: 837–846.
9. Skaug M A, Helland I, Solvoll K, and Saugstad O D (2001) Presence of ochratoxin A in human milk in relation to dietary intake. *Food Addit. Contam.* 18: 321–327.
10. Berndt W O, and Hayes A W (1979) In vivo and in vitro changes in renal function caused by ochratoxin A in the rat. *Toxicology* 12: 5–17.
11. Larsen J C, Hunt J, Perrin I, and Ruckenbauer P (2004) Workshop on trichothecenes with a focus on DON: summary report. *Toxicol. Lett.* 153: 1–22.
12. Furuse M, Fujita K, Hiiragi T, Fujimoto K, and Tsukita S (1998) Claudin-1 and -2: novel integral membrane proteins localizing at tight junctions with no sequence

- similarity to occludin. *J. Cell Biol.* 141: 1539–1550.
13. Furuse M, Hirase T, Itoh M, Nagafuchi A, Yonemura S, Tsukita S, and Tsukita S (1993) Occludin: a novel integral membrane protein localizing at tight junctions. *J. Cell Biol.* 123: 1777–1788.
  14. Martin-Padura I, Lostaglio S, Schneemann M, Williams L, Romano M, Fruscella P, Panzeri C, Stoppacciaro A, Ruco L, Villa A, Simmons D, and Dejana E (1998) Junctional adhesion molecule, a novel member of the immunoglobulin superfamily that distributes at intercellular junctions and modulates monocyte transmigration. *J. Cell Biol.* 142: 117–127.
  15. Ikenouchi J, Furuse M, Furuse K, Sasaki H, Tsukita S, and Tsukita S (2005) Tricellulin constitutes a novel barrier at tricellular contacts of epithelial cells. *J. Cell Biol.* 171: 939–945.
  16. Steed E, Rodrigues N T, Balda M S, and Matter K (2009) Identification of MarvelD3 as a tight junction-associated transmembrane protein of the occludin family. *BMC Cell Biol.* 10: 95.
  17. Gumbiner B, Lowenkopf T, and Apatira D (1991) Identification of a 160-kDa polypeptide that binds to the tight junction protein ZO-1. *Proc. Natl. Acad. Sci. U S A.* 88: 3460–3464.
  18. Haskins J, Gu L, Wittchen E S, Hibbard J, and Stevenson B R (1998) ZO-3, a novel member of the MAGUK protein family found at the tight junction, interacts with ZO-1 and occludin. *J. Cell Biol.* 141: 199–208.
  19. Stevenson B R, Siliciano J D, Mooseker M S, and Goodenough D A (1986) Identification of ZO-1: a high molecular weight polypeptide associated with the tight junction (zonula occludens) in a variety of epithelia. *J. Cell Biol.* 103: 755–766.
  20. Mineta K, Yamamoto Y, Yamazaki Y, Tanaka H, Tada Y, Saito K, Tamura A, Igarashi M, Endo T, Takeuchi K, and Tsukita S (2011) Predicted expansion of the claudin multigene family. *FEBS Lett.* 585: 606–612.
  21. Amasheh S, Schmidt T, Mahn M, Florian P, Mankertz J, Tavalali S, Gitter A H, Schulzke J D, and Fromm M (2005) Contribution of claudin-5 to barrier properties in tight junctions of epithelial cells. *Cell Tissue Res.* 321: 89–96.
  22. Furuse M, Hata M, Furuse K, Yoshida Y, Haratake A, Sugitani Y, Noda T, Kubo A, and Tsukita S (2002) Claudin-based tight junctions are crucial for the mammalian epidermal barrier: a lesson from claudin-1-deficient mice. *J. Cell Biol.* 156: 1099–1111.
  23. Milatz S, Krug S M, Rosenthal R, Gunzel D, Muller D, Schulzke J D, Amasheh S, and Fromm M (2010) Claudin-3 acts as a sealing component of the tight junction for ions of either charge and uncharged solutes. *Biochim. Biophys. Acta* 1798: 2048–2057.
  24. Van Itallie C M, Fanning A S, and Anderson J M (2003) Reversal of charge selectivity

- in cation or anion-selective epithelial lines by expression of different claudins. *Am. J. Physiol. Renal. Physiol.* 285: F1078–1084.
25. Amasheh S, Meiri N, Gitter A H, Schoneberg T, Mankertz J, Schulzke J D, and Fromm M (2002) Claudin-2 expression induces cation-selective channels in tight junctions of epithelial cells. *J. Cell Sci.* 115: 4969–4976.
  26. Gunzel D, Stuiver M, Kausalya P J, Haisch L, Krug S M, Rosenthal R, Meij I C, Hunziker W, Fromm M, and Muller D (2009) Claudin-10 exists in six alternatively spliced isoforms that exhibit distinct localization and function. *J. Cell Sci.* 122: 1507–1517.
  27. Inai T, Kamimura T, Hirose E, Iida H, and Shibata Y (2010) The protoplasmic or exoplasmic face association of tight junction particles cannot predict paracellular permeability or heterotypic claudin compatibility. *Eur. J. Cell Biol.* 89: 547–556.
  28. Tamura A, Hayashi H, Imasato M, Yamazaki Y, Hagiwara A, Wada M, Noda T, Watanabe M, Suzuki Y, and Tsukita S (2011) Loss of claudin-15, but not claudin-2, causes Na<sup>+</sup> deficiency and glucose malabsorption in mouse small intestine. *Gastroenterology* 140: 913–923.
  29. Van Itallie C M, Rogan S, Yu A, Vidal L S, Holmes J, and Anderson J M (2006) Two splice variants of claudin-10 in the kidney create paracellular pores with different ion selectivities. *Am. J. Physiol. Renal. Physiol.* 291: F1288–1299.
  30. Yu A S, Cheng M H, Angelow S, Gunzel D, Kanzawa S A, Schneeberger E E, Fromm M, and Coalson R D (2009) Molecular basis for cation selectivity in claudin-2-based paracellular pores: identification of an electrostatic interaction site. *J. Gen. Physiol.* 133: 111–127.
  31. Krug S M, Gunzel D, Conrad M P, Rosenthal R, Fromm A, Amasheh S, Schulzke J D, and Fromm M (2012) Claudin-17 forms tight junction channels with distinct anion selectivity. *Cell Mol. Life Sci.* 69: 2765–2778.
  32. Akbari P, Braber S, Gremmels H, Koelink P J, Verheijden K A, Garssen J, and Fink-Gremmels J (2014) Deoxynivalenol: a trigger for intestinal integrity breakdown. *FASEB J.* 28: 2414–2429.
  33. De Walle J V, Sergent T, Piront N, Toussaint O, Schneider Y J, and Larondelle Y (2010) Deoxynivalenol affects in vitro intestinal epithelial cell barrier integrity through inhibition of protein synthesis. *Toxicol. Appl. Pharmacol.* 245: 291–298.
  34. Lambert D, Padfield P J, McLaughlin J, Cannell S, and O'Neill C A (2007) Ochratoxin A displaces claudins from detergent resistant membrane microdomains. *Biochem. Biophys. Res. Commun.* 358: 632–636.
  35. McLaughlin J, Padfield P J, Burt J P, and O'Neill C A (2004) Ochratoxin A increases permeability through tight junctions by removal of specific claudin isoforms. *Am. J. Physiol. Cell Physiol.* 287: C1412–1417.

36. Pinton P, Braicu C, Nougayrede J P, Laffitte J, Taranu I, and Oswald I P (2010) Deoxynivalenol impairs porcine intestinal barrier function and decreases the protein expression of claudin-4 through a mitogen-activated protein kinase-dependent mechanism. *J. Nutr.* 140: 1956–1962.
37. Pinton P, Nougayrede J P, Del Rio J C, Moreno C, Marin D E, Ferrier L, Bracarense A P, Kolf-Clauw M, and Oswald I P (2009) The food contaminant deoxynivalenol, decreases intestinal barrier permeability and reduces claudin expression. *Toxicol. Appl. Pharmacol.* 237: 41–48.
38. Pinton P, Tsybulskyy D, Lucioli J, Laffitte J, Callu P, Lyazhri F, Grosjean F, Bracarense A P, Kolf-Clauw M, and Oswald I P (2012) Toxicity of deoxynivalenol and its acetylated derivatives on the intestine: differential effects on morphology, barrier function, tight junction proteins, and mitogen-activated protein kinases. *Toxicol. Sci.* 130: 180–190.
39. Springler A, Hessenberger S, Schatzmayr G, and Mayer E (2016) Early activation of MAPK p44/42 is partially involved in DON-induced disruption of the intestinal barrier function and tight junction network. *Toxins (Basel)* 8: E264.
40. Lu Z, Ding L, Lu Q, and Chen Y H (2013) Claudins in intestines: Distribution and functional significance in health and diseases. *Tissue Barriers* 1: e24978.
41. Escaffit F, Boudreau F, and Beaulieu J F (2005) Differential expression of claudin-2 along the human intestine: Implication of GATA-4 in the maintenance of claudin-2 in differentiating cells. *J. Cell Physiol.* 203: 15–26.
42. Holmes J L, Van Itallie C M, Rasmussen J E, and Anderson J M (2006) Claudin profiling in the mouse during postnatal intestinal development and along the gastrointestinal tract reveals complex expression patterns. *Gene Expr. Patterns* 6: 581–588.
43. Franks L M, and Hemmings V J (1978) A cell line from an induced carcinoma of mouse rectum. *J. Pathol.* 124: 35–38.
44. Inai T, Sengoku A, Hirose E, Iida H, and Shibata Y (2008) Comparative characterization of mouse rectum CMT93-I and -II cells by expression of claudin isoforms and tight junction morphology and function. *Histochem. Cell Biol.* 129: 223–232.
45. Prasad S, Mingrino R, Kaukinen K, Hayes K L, Powell R M, MacDonald T T, and Collins J E (2005) Inflammatory processes have differential effects on claudins 2, 3 and 4 in colonic epithelial cells. *Lab. Invest.* 85: 1139–1162.
46. Inai T, Kitagawa N, Hatakeyama Y, Ikebe T, Iida H, and Fujita M (2013) Inhibition of extracellular signal-regulated kinase downregulates claudin-2 expression and alters paracellular permeability in mouse rectum CMT93-II cells. *Tissue Cell* 45: 175–182.
47. Body-Malapel M, Dharancy S, Berrebi D, Louvet A, Hugot J P, Philpott D J,

- Giovannini M, Chareyre F, Pages G, Gantier E, Girardin SE, Garcia I, Hudault S, Conti F, Sansonetti PJ, Chamaillard M, Desreumaux P, Dubuquoy L, and Mathurin P (2008) NOD2: a potential target for regulating liver injury. *Lab. Invest.* 88: 318–327.
48. Liu T, Shi Y, Du J, Ge X, Teng X, Liu L, Wang E, and Zhao Q (2016) Vitamin D treatment attenuates 2,4,6-trinitrobenzene sulphonic acid (TNBS)-induced colitis but not oxazolone-induced colitis. *Sci. Rep.* 6: 32889.
49. Jimenez F R, Belgique S T, Lewis J B, Albright S A, Jones C M, Howell B M, Mika A P, Jergensen T R, Gassman J R, Morris R J, Arroyo JA, and Reynolds PR (2015) Conditional pulmonary over-expression of Claudin 6 during embryogenesis delays lung morphogenesis. *Int. J. Dev. Biol.* 59: 479–485.
50. Fan W, Xu L, Ren L, Qu H, Li J, Liang J, Liu W, Yang L, and Luo T (2014) Functional characterization of canine interferon-lambda. *J. Interferon Cytokine Res.* 34: 848–857.
51. Garcia-Hernandez V, Flores-Maldonado C, Rincon-Heredia R, Verdejo-Torres O, Bonilla-Delgado J, Meneses-Morales I, Gariglio P, and Contreras R G (2015) EGF regulates claudin-2 and -4 expression through Src and STAT3 in MDCK cells. *J. Cell Physiol.* 230: 105–115.
52. Inai T, Kobayashi J, and Shibata Y (1999) Claudin-1 contributes to the epithelial barrier function in MDCK cells. *Eur. J. Cell Biol.* 78: 849–855.
53. Alexandre M D, Lu Q, and Chen Y H (2005) Overexpression of claudin-7 decreases the paracellular Cl<sup>-</sup> conductance and increases the paracellular Na<sup>+</sup> conductance in LLC-PK1 cells. *J. Cell Sci.* 118: 2683–2693.
54. Maresca M, Yahi N, Younes-Sakr L, Boyron M, Caporiccio B, and Fantini J (2008) Both direct and indirect effects account for the pro-inflammatory activity of enteropathogenic mycotoxins on the human intestinal epithelium: stimulation of interleukin-8 secretion, potentiation of interleukin-1beta effect and increase in the transepithelial passage of commensal bacteria. *Toxicol. Appl. Pharmacol.* 228: 84–92.
55. Romero A, Ares I, Ramos E, Castellano V, Martinez M, Martinez-Larranaga M R, Anadon A, and Martinez M A (2016) Mycotoxins modify the barrier function of Caco-2 cells through differential gene expression of specific claudin isoforms: Protective effect of illite mineral clay. *Toxicology* 353–354: 21–33.
56. Rumora L, Domijan A M, Zanic Grubisic T, and Segvic Klaric M (2014) Differential activation of MAPKs by individual and combined ochratoxin A and citrinin treatments in porcine kidney PK15 cells. *Toxicon* 90: 174–183.
57. Furuse M, Furuse K, Sasaki H, and Tsukita S (2001) Conversion of zonulae occludentes from tight to leaky strand type by introducing claudin-2 into Madin-Darby canine kidney I cells. *J. Cell Biol.* 153: 263–272.
58. Kasuga F, Hara-Kudo Y, Saito N, Kumagai S, and Sugita-Konishi Y (1998) In vitro

- effect of deoxynivalenol on the differentiation of human colonic cell lines Caco-2 and T84. *Mycopathologia* 142: 161–167.
59. Maresca M, Mahfoud R, Pfohl-Leszkowicz A, and Fantini J (2001) The mycotoxin ochratoxin A alters intestinal barrier and absorption functions but has no effect on chloride secretion. *Toxicol. Appl. Pharmacol.* 176: 54–63.
  60. Diesing A K, Nossol C, Danicke S, Walk N, Post A, Kahlert S, Rothkotter H J, and Kluess J (2011) Vulnerability of polarised intestinal porcine epithelial cells to mycotoxin deoxynivalenol depends on the route of application. *PLoS One* 6: e17472.
  61. Zakrzewski S S, Richter J F, Krug S M, Jebautzke B, Lee I F, Rieger J, Sachtleben M, Bondzio A, Schulzke J D, Fromm M, and Gunzel D (2013) Improved cell line IPEC-J2, characterized as a model for porcine jejunal epithelium. *PLoS One* 8: e79643.
  62. Schierack P, Nordhoff M, Pollmann M, Weyrauch K D, Amasheh S, Lodemann U, Jores J, Tachu B, Kleta S, Blikslager A, Tedin K, and Wieler LH (2006) Characterization of a porcine intestinal epithelial cell line for in vitro studies of microbial pathogenesis in swine. *Histochem. Cell Biol.* 125: 293–305.
  63. Michikawa H, Fujita-Yoshigaki J, and Sugiya H (2008) Enhancement of barrier function by overexpression of claudin-4 in tight junctions of submandibular gland cells. *Cell Tissue Res.* 334: 255–264.
  64. Van Itallie C, Rahner C, and Anderson J M (2001) Regulated expression of claudin-4 decreases paracellular conductance through a selective decrease in sodium permeability. *J. Clin. Invest* 107: 1319–1327.
  65. Hou J, Renigunta A, Yang J, and Waldegger S (2010) Claudin-4 forms paracellular chloride channel in the kidney and requires claudin-8 for tight junction localization. *Proc. Natl. Acad. Sci. U S A* 107: 18010–18015.
  66. Sas D, Hu M, Moe O W, and Baum M (2008) Effect of claudins 6 and 9 on paracellular permeability in MDCK II cells. *Am. J. Physiol. Regul. Integr. Comp. Physiol.* 295: R1713–1719.
  67. Luciola J, Pinton P, Callu P, Laffitte J, Grosjean F, Kolf-Clauw M, Oswald I P, and Bracarense A P (2013) The food contaminant deoxynivalenol activates the mitogen activated protein kinases in the intestine: interest of ex vivo models as an alternative to in vivo experiments. *Toxicon* 66: 31–36.
  68. Pestka J J (2008) Mechanisms of deoxynivalenol-induced gene expression and apoptosis. *Food Addit. Contam. Part A Chem. Anal. Control Expo. Risk Assess.* 25: 1128–1140.
  69. Kinugasa T, Sakaguchi T, Gu X, and Reinecker H C (2000) Claudins regulate the intestinal barrier in response to immune mediators. *Gastroenterology* 118: 1001–1011.
  70. Singh A B, and Harris R C (2004) Epidermal growth factor receptor activation

- differentially regulates claudin expression and enhances transepithelial resistance in Madin-Darby canine kidney cells. *J. Biol. Chem.* 279: 3543–3552.
71. Dukes J D, Whitley P, and Chalmers A D (2012) The PIKfyve inhibitor YM201636 blocks the continuous recycling of the tight junction proteins claudin-1 and claudin-2 in MDCK cells. *PLoS One* 7: e28659.
  72. Lu R, Johnson D L, Stewart L, Waite K, Elliott D, and Wilson J M (2014) Rab14 regulation of claudin-2 trafficking modulates epithelial permeability and lumen morphogenesis. *Mol. Biol. Cell* 25: 1744–1754.
  73. Nighot P K, Hu C A, and Ma T Y (2015) Autophagy enhances intestinal epithelial tight junction barrier function by targeting claudin-2 protein degradation. *J. Biol. Chem.* 290: 7234–7246.

**Table 1.** Summary of effects of deoxynivalenol, ochratoxin A, and citrinin on the intestinal cell lines, jejunal explants or MDCK II cells.

Cells	Conc. ( $\mu$ M)	TER	Flux	WB		IF	qPCR	Ref
deoxynivalenol								
Caco-2	0.34	↓	↑ <sup>1</sup>					58
	100	↓	↑ <sup>2,3</sup>					54
	30–100	↓	↑ <sup>2</sup>	CL3 → CL4 ↓		CL3 → CL4 ↓		37
	1.69	↓	↑ <sup>4</sup>	CL4 ↓				33
	1.39–12.5	↓	↑ <sup>1,2</sup>	CL1 ↓ CL3 ↓ CL4 ↓		CL1 ↓ CL3 ↓ CL4 ↓	CL1 ↑ CL3 ↑ CL4 ↑	32
T84	0.34	↓	↑ <sup>1</sup>					58
IPEC-1	5–30	↓	↑ <sup>2</sup>	CL3 ↓ CL4 ↓		CL3 ↓ CL4 ↓		37
	30	↓	↑ <sup>2</sup>	CL4 ↓	P-ERK ↑	CL4 ↓	CL4 ↑	36
	30	↓		CL3 ↓ CL4 ↓	P-ERK ↑ P-p38 ↑ P-JNK ↑	CL3 ↓ CL4 ↓		38
IPEC-J2	6.76	↓		CL3 ↓		CL3 ↓		60
	5–20	↓		CL1 ↓ CL3 ↓ CL4 →	P-ERK ↑ P-p38 ↑			39

Explants	10	↓						67
CMT93-II	1	↑	→ <sup>5</sup>	CL2 ↓ CL4 ↓ CL6 ↓	P-ERK ↓ P-p38 ↓	CL2 ↓ CL4 → CL6 →	CL2 ↓ CL4 ↑ CL6 →	*
MDCK II	1			CL2 ↓		CL2 ↓	CL2 ↓	*
ochratoxin A								
Caco-2	17–40	↓						59
	50–100	↓	↑ <sup>2,6</sup>	CL1 → CL3 ↓ CL4 ↓		CL1 → CL3 ↓ CL4 ↓		35
	100	↓		CL1 → CL3 ↓ CL4 ↓				34
	100	↓	↑ <sup>2,3</sup>					54
	1–100	↓					CL3 ↓ CL4 ↓	55
HT-29-D4	6–10	↓						59
CMT93-II	40	↑	→ <sup>5</sup>	CL2 ↓ CL4 ↓ CL6 →	P-ERK → P-p38 ↑	CL2 ↓ CL4 ↓ CL6 →	CL2 ↓ CL4 ↓ CL6 ↓	*
MDCK II	10			CL2 →		CL2 →	CL2 ↓	*
citrinin								
CMT93-II	50	↑	→ <sup>5</sup>	CL2 ↓ CL4 → CL6 →	P-ERK ↓ P-p38 ↑	CL2 ↓ CL4 → CL6 →	CL2 ↓ CL4 ↓ CL6 ↓	*

---

Conc.: concentration, WB: western blotting, IF: immunofluorescence, Ref: reference number, CL: claudin, P-ERK: phosphorylated ERK, P-p38: phosphorylated p38, P-JNK: phosphorylated JNK, ↑: increase, ↓: decrease, →: steady, \*the present study. Tracers of flux: <sup>1</sup>Lucifer yellow, <sup>2</sup>4 kD FITC-dextran, <sup>3</sup>Horseshoe radish peroxidase, <sup>4</sup>Mannitol, <sup>5</sup>Fluorescein, <sup>6</sup>10 kD FITC-dextran.

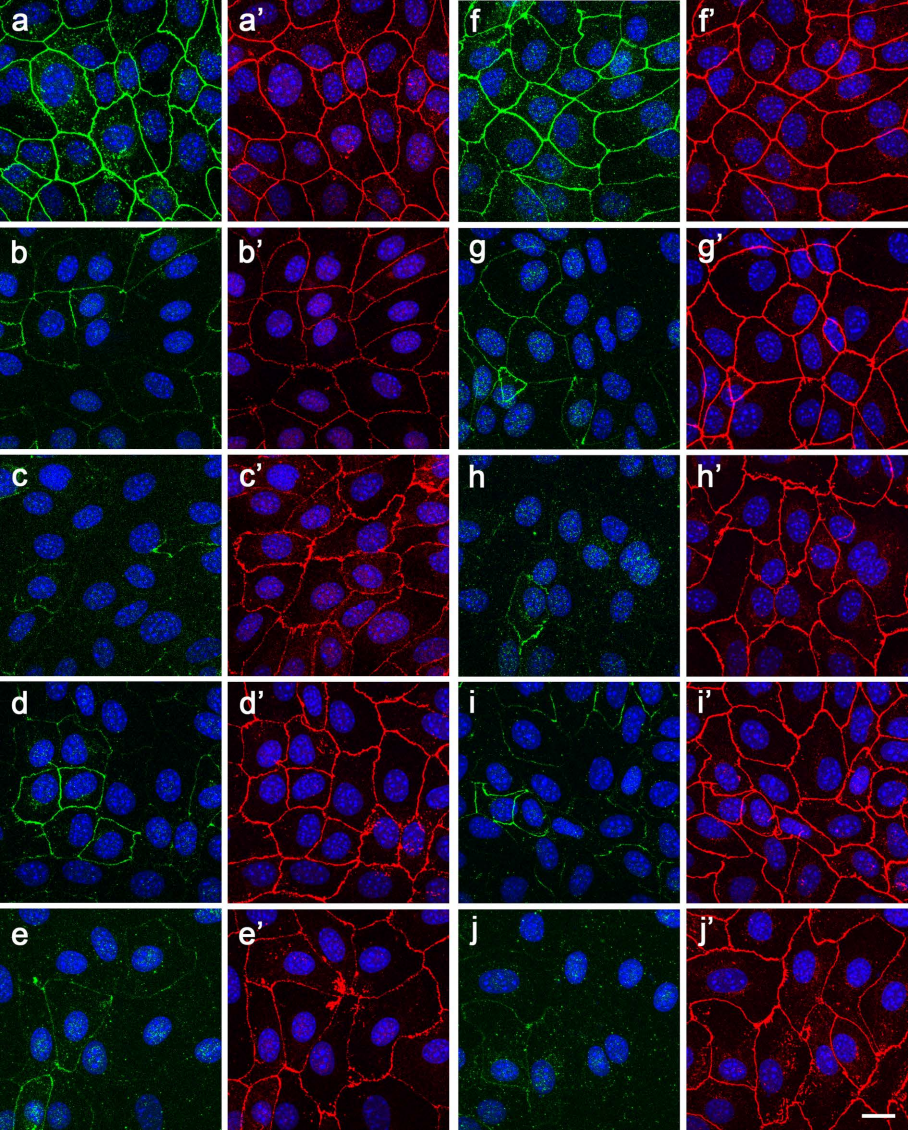


**Fig. 1.** Treatment with OTA, CTN, DON, and U0126 reduces claudin-2 expression at sites of cell-cell contact between CMT93-II cells derived from the mouse rectum. Confluent CMT93-II cells were treated with vehicle (a, a', f, f'), 40  $\mu$ M OTA (b, b', g, g'), 50  $\mu$ M CTN (c, c', h, h'), 1  $\mu$ M DON (d, d', i, i'), or 20  $\mu$ M U0126 (e, e', j, j') for 36 h. The cells were doubly stained with antibodies against claudin-2 (a–e, green) and claudin-4 (a'–e', red) or antibodies against claudin-2 (f–j, green) and claudin-6 (f'–j', red). The nuclei were stained with DAPI (blue). The image was a stack of six *x*–*y* sections recorded at 0.48- $\mu$ m intervals from base to apex by confocal microscopy. Scale bar: 20  $\mu$ m for all images.

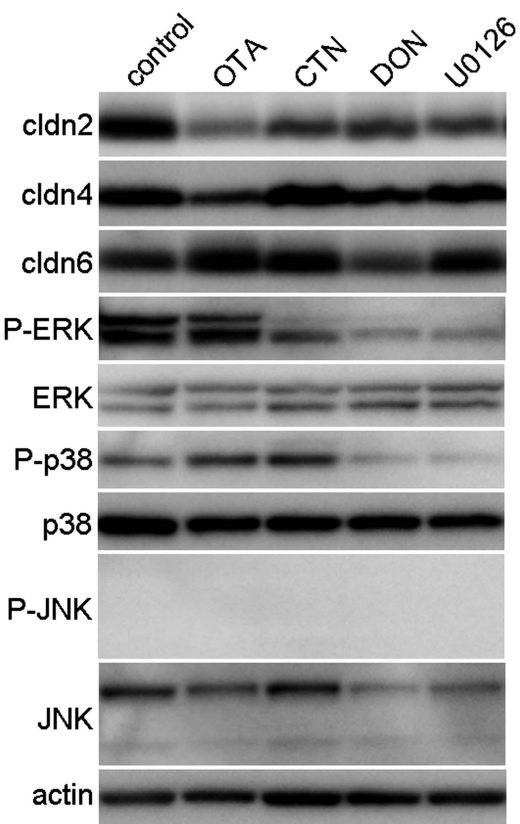


**Fig. 2.** Immunoblot analysis of claudins and MAPKs in CMT93-II cells. Confluent CMT93-II cells treated with 40  $\mu$ M OTA, 50  $\mu$ M CTN, 1  $\mu$ M DON, 20  $\mu$ M U0126, or 0.1% DMSO (vehicle) for 36 h were lysed, fractionated by SDS-PAGE, and transferred onto PVDF membranes. Immunoblotting was performed using antibodies against claudin-2, -4, and -6, P-ERK, ERK, P-p38, p38, P-JNK, JNK, and  $\beta$ -actin. Membranes were reprobbed after stripping primary and secondary antibodies.

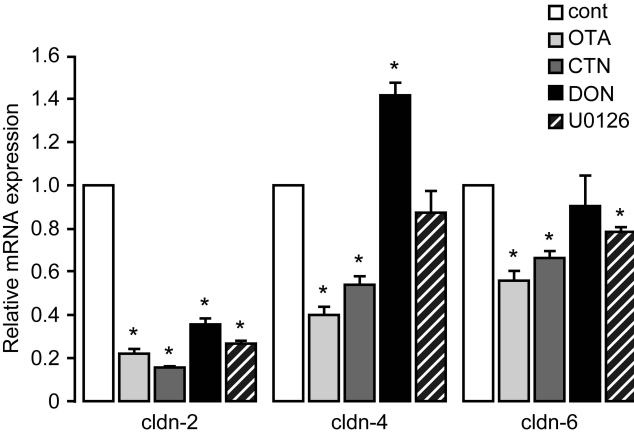
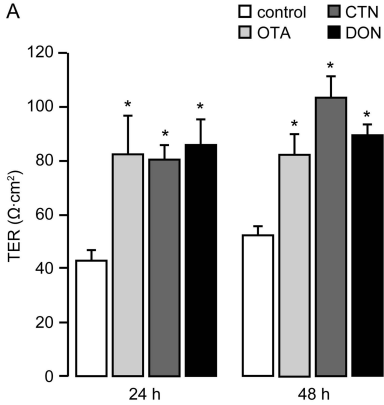


**Fig. 3.** qPCR analysis of mRNA expression levels of claudin (cldn)-2, -4, and -6 in CMT93-II cells. Confluent CMT93-II cells were treated with 40  $\mu$ M OTA, 50  $\mu$ M CTN, 1  $\mu$ M DON, 20  $\mu$ M U0126, or 0.1% DMSO (vehicle) for 36 h. Total RNA isolated from these treated cells was reverse transcribed to synthesize cDNA, which was used for PCR amplification. The reference gene,  $\beta$ -actin, was used as a control. Data represent the mean  $\pm$  SEM of two independent experiments performed in triplicate. \*P < 0.05 vs control.

A



B

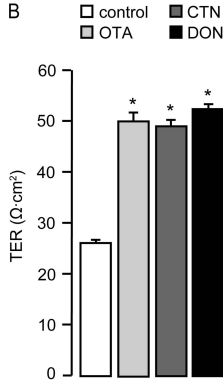


**Fig. 4.** Treatment with OTA, CTN, and DON increases the TER of the CMT93-II monolayer by reducing paracellular permeability for Na<sup>+</sup>. CMT93-II cells grown on inserts were treated with 100 μM OTA, 125 μM CTN, 2.5 μM DON, or 0.25% DMSO (vehicle) in the apical compartment. (A) TER of the CMT93-II monolayer in DMEM containing 10% FBS was measured at 24 and 48 h after addition of mycotoxins. (B) After measurement of TER at 48 h, cells were washed three times with P<sub>Na</sub> buffer and TER was measured in P<sub>Na</sub> buffer. Data represent the mean ± SEM of two independent experiments performed in triplicate. \*P < 0.05 vs control.

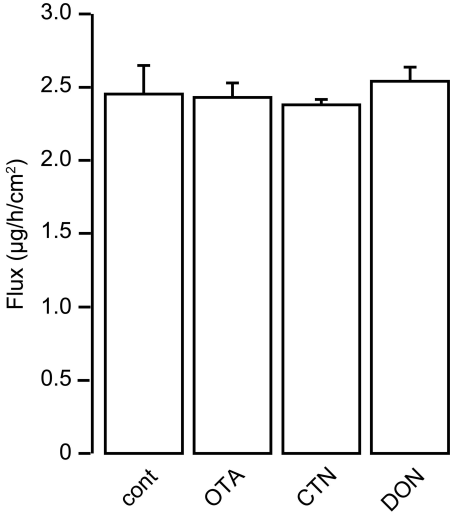


**Fig. 5.** Treatment with OTA, CTN, and DON does not alter the permeability of the CMT93-II monolayer. CMT93-II cells grown on inserts were treated with 100  $\mu$ M OTA, 125  $\mu$ M CTN, 2.5  $\mu$ M DON, or 0.25% DMSO (vehicle) in the apical compartment. After treatment with mycotoxins for 48 h, the culture medium was replaced with P buffer with or without 30  $\mu$ g/mL fluorescein in the apical or basal compartment, respectively, and further cultured for 2 h. The P buffer from the lower compartment was then collected and flux of fluorescein was measured. Data represent the mean  $\pm$  SEM of two independent experiments performed in triplicate. \*P < 0.05 vs control.

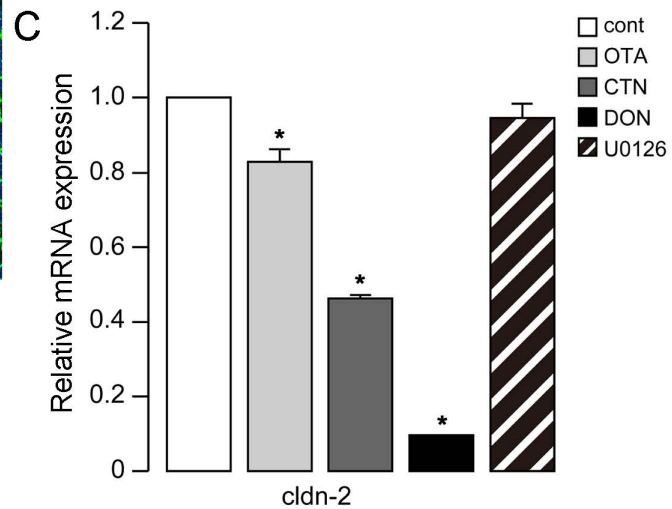
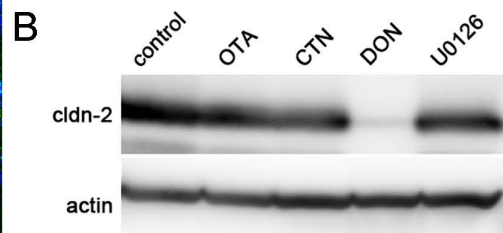
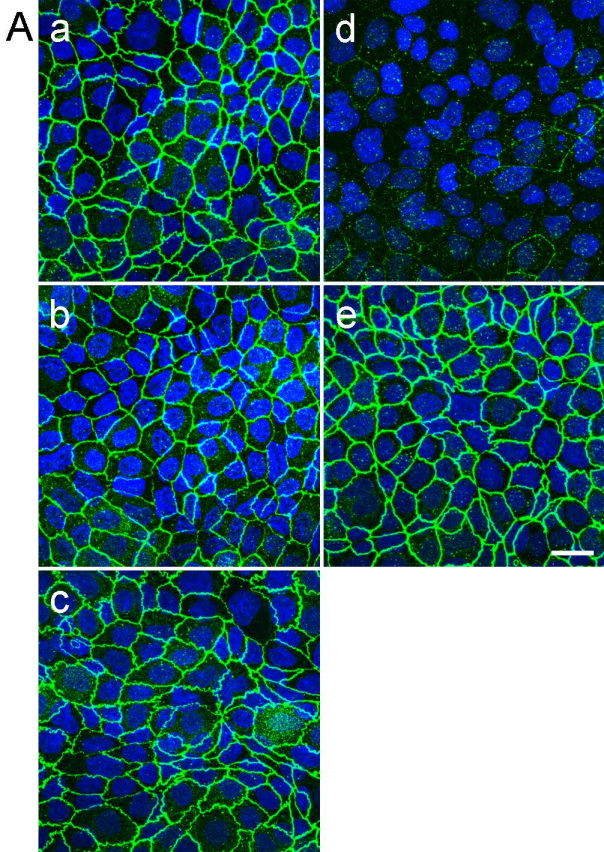


**Fig. 6.** Effect of OTA, CTN, DON, and U0126 on localization, protein expression, and mRNA expression of claudin-2 in MDCK II cells derived from the renal tubule. Confluent MDCK II cells were treated with vehicle (a), 10  $\mu$ M OTA (b), 50  $\mu$ M CTN (c), 1  $\mu$ M DON (d), or 20  $\mu$ M U0126 (e) for 36 h. (A) The treated cells were stained with antibodies for claudin-2 (green). The nuclei were stained with DAPI (blue). The image was a stack of six *x-y* sections recorded at 0.48- $\mu$ m intervals from base to apex by confocal microscopy. Scale bar: 20  $\mu$ m for all images. (B) The treated cells were lysed, fractionated by SDS-PAGE, and transferred onto PVDF membranes. Immunoblotting was performed using antibodies against claudin-2 and  $\beta$ -actin. After primary and secondary antibodies were stripped from the blots, the membranes were reprobbed. (C) Total RNA isolated from these treated cells was reverse transcribed to synthesize cDNA, which was amplified by PCR. The reference gene,  $\beta$ -actin, was used as the control. Data represent the mean  $\pm$  SEM of two independent experiments performed in triplicate. \* $P < 0.05$  vs control.